

Sex steroids modulate morphological and functional features of the bovine oviduct

Angela Maria Gonella-Diaza¹ · Fernando Silveira Mesquita² · Kauê Ribeiro da Silva¹ · Júlio Cesar de Carvalho Balieiro¹ · Nilton Pedro dos Santos³ · Guilherme Pugliesi³ · Ricardo de Francisco Strefezzi³ · Mario Binelli¹

Received: 15 February 2017 / Accepted: 4 July 2017 / Published online: 2 August 2017
© Springer-Verlag GmbH Germany 2017

Abstract In cattle, the oviduct plays a major role in the reproductive process; however, molecular control of oviduct receptivity to the embryo is poorly understood. A model for receptivity based on size of the pre-ovulatory follicle (POF) was used to compare oviductal morphology, cellular proliferation, and candidate transcript abundance. Growth of the POF of Nelore (*Bos indicus*) cows was manipulated to produce two groups: a large POF-large corpus luteum (CL) group (LF-LCL; greater receptivity) and a small POF-small CL group (SF-SCL). Samples of the ampulla and isthmus ipsilateral and contralateral to CL were collected 4 days after GnRH-induced ovulation. Tissues were either embedded in paraffin for Harris-Hematoxylin and Eosin and periodic acid-Schiff staining and KI67 immunostaining, followed by morphological analyses, or stored at -80°C for RNA extraction, cDNA synthesis, and qPCR analyses. The effects of group (LF-LCL and SF-SCL), region (ampulla and isthmus), and side (ipsilateral and contralateral) were analyzed using three-way nested ANOVA. The ipsilateral ampulla of the LF-LCL group presented more primary mucosal folds, a greater mucosal-folding grade and luminal perimeter, and more secretory cells and proliferating cells when compared with the ampulla of the SF-SCL group and with the contralateral ampulla of both groups. There were no morphological differences in the

isthmus between groups and sides. Changes in transcript abundance are suggestive of LF-LCL-stimulated secretory activity. In summary, ovulation of a larger POF generates a periovulatory endocrine milieu that modulates morphological and functional features of the bovine oviduct which may support embryo survival and development.

Keywords Ampulla · Isthmus · Secretory cells · Receptivity · Cellular proliferation

Introduction

The oviduct, the anterior-most tubular segment of the female reproductive tract, is composed of three specialized regions, the infundibulum, ampulla, and isthmus, each with distinct morphological, cellular, molecular and functional characteristics (Hunter 1998, 2012; Leese 1988). The oviduct must provide a suitable environment for the transport of gametes, fertilization, and early embryo development (Besenfelder et al. 2012; Hunter 2012). During pre-natal development of the reproductive tract, the oviductal lumen is defined by a fairly flat epithelial lining, without appreciable folding. The complexity of mucosal folds starts to develop only in the postnatal life, and, in the adult animal, oviductal folds develop a complex organization exhibiting primary, secondary, and tertiary folds (Agduhr 1927; Kennigott and Sinowatz 2007; Konishi et al. 1987). At this point, the oviductal epithelium forms longitudinal folds that increase the epithelial surface area, allowing for an improved interaction with gametes and embryos during their transit through the organ. However, this organization varies according to the oviductal region (Abe 1996; Bacha and Bacha 2012) and the phase of the estrous cycle (McDaniel et al. 1968; Mokhtar 2015; Restall 1966). In general, the infundibulum and ampulla present greater numbers

✉ Mario Binelli
binelli@usp.br

¹ Faculdade de Medicina Veterinária e Zootecnia, Universidade de São Paulo, Pirassununga, São Paulo, Brazil

² Curso de Medicina Veterinária, Universidade Federal do Pampa, Uruguaiana, Rio Grande do Sul, Brazil

³ Faculdade de Zootecnia e Engenharia de Alimentos, Universidade de São Paulo, Pirassununga, São Paulo, Brazil

and complexity of folds than the isthmus; additionally, during estrus, the number of folds, as well as their degree of folding, is increased (Restall 1966). Furthermore, the oviductal epithelium contains two main cell types: ciliated and secretory cells. Ciliated cells are involved in sperm capacitation, transport of sperm cells and embryo, and to some extent, secretion of molecules into the lumen (Donnez et al. 1985; Hunter 2012). On the other hand, unlike ciliated cells, secretory cells have their cellular machinery specifically organized for the synthesis and secretion of substances into the oviductal lumen (Brower and Anderson 1969; Gandolfi et al. 1989). The proportion of these cells varies across the oviductal regions; with the ampulla exhibiting greater secretory activity compared to the other two regions owing to its greater proportion of secretory cells (Buhi et al. 2000).

Several studies have shown that appropriate timing and prominence of sex-steroid hormones is important to ensure maternal receptivity (Ashworth et al. 1989; Demetrio et al. 2007; Morris and Diskin 2008). It has also been established that cows ovulating larger follicles can attain greater proestrus estradiol (E2) plasma concentrations, form a larger corpus luteum (CL), and produce greater progesterone (P4) concentrations during early diestrus (Demetrio et al. 2007; Mesquita et al. 2014; Peres et al. 2009; Vasconcelos et al. 2001). Furthermore, cows with such a periovulatory endocrine profile present increased fertility when compared to cows ovulating smaller follicles and forming smaller CLs (Pugliesi et al. 2016). This increase in fertility is associated with changes in the endometrial (Mesquita et al. 2015) and oviductal (Gonella-Diaza et al. 2015) transcriptome. However, very little is known about whole-organ, cellular and molecular mechanisms that could regulate oviductal functions, and that are associated with fertility. In a recent study, Gonella-Diaza et al. 2015 used an experimental model to manipulate the pre-ovulatory follicle growth producing two groups of animals with distinctly different endocrine and ovarian phenotypes, the large follicle, large CL (LF-LCL) and the small follicle, small CL (SF-SCL) groups. On day 4 of the estrous cycle, LF-LCL cows presented 692 and 590 differentially expressed genes in the ampulla and isthmus, respectively, when compared to SF-SCL cows. Among these differentially expressed genes, several enriched cellular and metabolic processes such as branching morphogenesis, cellular proliferation and secretion were identified. However, whether such changes in transcript abundance resulted in phenotypic changes that could be related to oviductal functions remains unknown. Enrichment of transcripts associated with the aforementioned processes in the oviducts of LF-LCL cows suggests an increased proliferative activity of oviductal luminal epithelium, leading to folding and, consequently, increased surface area of the epithelial lining and secretion capacity. This phenotype might represent an advantage for the oviductal environment of cows via the local circulation of a more

favorable endocrine profile arising from the ovulation of larger follicles and CLs, thus resulting in improved production and secretion of nutrients and growth factors by the oviduct, ultimately leading to greater embryo quality and development potential (Ahumada et al. 2013; Wetscher et al. 2005). Thus, the objectives of this study were to compare (1) the oviduct morphology, (2) abundance of transcripts related to branching morphogenesis and cellular secretion, and (3) cellular proliferation between cows treated to ovulate larger or smaller follicles.

Materials and methods

Animal handling, reproductive management, and tissue processing

All animal procedures were approved by the Ethics and Animal Handling Committee of the School of Veterinary Medicine and Animal Science of the University of São Paulo (USP) in São Paulo, Brazil (CEUA/FMVZ; protocols numbers 2281–2011 and 4,293,160,916). The hormonal manipulation procedures described here have been validated and previously published (Gonella-Diaza et al. 2015; Mesquita et al. 2014, 2015). Briefly, prior to starting the experiment, 56 multiparous and non-lactating Nelore cows (*Bos indicus*) were selected, kept in grazing conditions (*Brachiaria brizantha* pasture), and supplemented with mineralized salt to fulfill their maintenance requirements. After a gynecological examination, cows were selected according to three criteria: no gross reproductive abnormalities, a body condition score between 3 and 4 (0, emaciated; 5, obese), and normal estrous cyclic activity.

Animals were randomly divided into two groups: LF-LCL and SF-SCL. Briefly, animals were pre-synchronized by intramuscular injection of GnRH agonist (1 µg of buserelin acetate; Sincroforte; Ouro Fino, Cravinhos, Brazil) and, 7 days later an injection of Prostaglandin F2 alpha analog (PGF; 0.5 mg of sodium cloprostenol; Sincrocio; Ouro Fino). Onb this day [day –20 (D-20)] animals received an ESTROTECT Heat detector patch (Rockway, Spring Valley, WI, USA) and estrus detection was performed twice daily from D-20 to D-10. Only animals with a fresh, PGF responsive CL (at least 5 days old) on D-10 stayed in the experiment. The remaining cows ($n = 41$) received a new intravaginal P4-releasing device (1 g; Sincrogest; Ouro Fino) on D-10 and an intramuscular injection of 2 mg E2 benzoate (Sincrodiol; Ouro Fino). Only cows of LF-LCL group received an im injection of PGF. P4-releasing devices were removed after 8.25 and 8.75 days in the LF-LCL and SF-SCL groups, respectively. The differential animal handling (PGF injection at the time of P4-device insertion and timing of device removal) during the synchronization protocol was designed to enable animals of the LF-LCL

group: (1) to develop a new follicular wave under a low P4 environment, and (2) to have more time to grow the preovulatory follicle during the proestrus. All animals received two PGF injections 6 h apart at P4 device removal. Ovulation was induced by an injection of 10 µg Buserelin on D0 (Sincroforte; Ouro Fino). Animals that responded to treatments were slaughtered on D4 after induction of ovulation (LF-LCL, $n = 13$; SF-SCL, $n = 10$).

Immediately after slaughter, the reproductive tract was transported on ice to the laboratory where the oviducts ipsilateral and contralateral to the ovary containing the CL were identified and dissected to obtain samples of ampulla and isthmus (Fig. 1). Two sub-samples were extracted from each oviductal region. These sub-samples were either fixed in buffered formalin or frozen in liquid nitrogen for histological or molecular analyses, respectively.

Histological analysis

Freshly dissected tissues remained in formalin for 24 h, were then dehydrated in a gradient of increasing ethanol concentrations, and cleared in a gradient of increasing concentrations of xylene before embedding in paraffin. Cross-sections were obtained at 4 µm thickness and from each sample; at least 5 non-consecutive sections, 8 µm apart, were obtained. Three sections were stained with Harris-Hematoxylin and Eosin (H&E), and two were stained with periodic acid-Schiff (PAS). The H&E stained sections were photographed using a stereomicroscope coupled to a digital camera and a computer with specialized software to capture the entire tissue section in the same image. PAS-stained luminal epithelium tissue sections were photographed with an optical microscope (Zeiss Axioplan 2; Zeiss, Oberkochen, Germany) coupled to a digital camera (Zeiss MC 80 DX; Zeiss) using $\times 100$ magnification with oil immersion. Initially, the pictures were analyzed to assess the quality and integrity of the tissue sample. Samples lacking unimpaired structural layer (tunica mucosa, tunica muscularis, and/or tunica serosa) or with strong signals of epithelial detachment were discarded. The remaining samples ($n = 28$) were used to perform the following analyses. The thickness (µm) of the tunica mucosa and tunica muscularis was determined using images of the H&E-stained sections loaded on Image Pro Plus 4.5 software (Media Cybernetics, Silver Spring, USA), (Fig. 2a and b, respectively). For each tissue sample, this procedure was performed 5 times in each of three non-consecutive tissue sections. The arithmetic mean of the 15 values was used for statistical analysis.

Using images of H&E-stained sections, the numbers of primary (Fig. 2c) and secondary (Fig. 2d) folds were counted using the “Cell Counter” plugin of ImageJ 1.48 software (National Institutes of Health, Bethesda, USA). For each tissue sample, this procedure was performed in three non-

consecutive sections and The arithmetic mean of the values was used for statistical analysis. The ratio of the number of secondary folds divided by the number of primary folds was assessed as a new variable named the folding grade. Due to the absence of tertiary folds in all isthmus samples, this variable was not considered in the study.

In the H&E-stained sections, the “trace-wand” tool of the Image Pro Plus software was used to draw the luminal epithelial lining. Tissue fragments that were detached from the luminal epithelium were ignored (Fig. 2e). For each tissue sample, this procedure was repeated on three non-consecutive tissue sections and the arithmetic mean of the three values was used for statistical analysis.

Images of PAS-stained tissue sections were loaded on the ImageJ software and the number of ciliated and secretory cells of the luminal epithelium was determined using the “Cell Counter” plugin. In order to identify each cell type, the following morphological characteristics were considered: the presence of cilia, the presence of cytoplasmic protrusions and PAS-positive granules in the secretory cells, as well as the position of the nuclei: basal for secretory cells and apical for ciliated cells (Fig. 3). Counting was continued until a total of 500 cells per sample were counted.

Determination of cellular proliferation

Paraffin-embedded oviductal samples were stained with antibodies against KI67 in order to identify proliferating oviductal luminal epithelial cells. Four-µm-thick tissue sections were deparaffinized in xylene and rehydrated in an ethanol series. These sections were then subjected to antigen retrieval by pressure cooking in citrate buffer (10 mM citric acid, pH 6.0), preheated to 80 °C for 1 min, allowed to cool for 20 min, and rinsed with PBS (1.09 g of Na₂HPO₄ anhydrous, 0.32 g of NaH₂PO₄ anhydrous, 9 g of NaCl, 1 ml of Tween20, 1000 ml of distilled water, pH 7.4). Endogenous peroxidase activity was blocked by incubation with Peroxidase Block kit (code K0679; Dako, Denmark) for 15 min at room temperature. After 3 consecutive washes with PBS, slides were incubated with Protein Block (Code X0909; Dako). Immediately, slides were incubated with monoclonal mouse anti-human KI67 primary antibody, Clone MIB-1 (code M7240; Dako) (Chanrota et al. 2017; Mesquita et al. 2015; Yoshioka et al. 2013), diluted in PBS (1:100, which corresponds to 0.52 µg/ml). Negative control slides were incubated with normal mouse IgG (sc-2025; Santa Cruz Biotechnology, Santa Cruz, CA, USA) with the same concentration of primary antibody. Both incubations were performed overnight at 4 °C. After the PBS wash series, slides were incubated with Advance Kit (Code K4069; Dako) for 15 min at room temperature with the HRP link and then with the HRP enzyme. After washing with PBS, 3,3-diaminobenzidine tetrahydrochloride (K3468; Dako) was used as

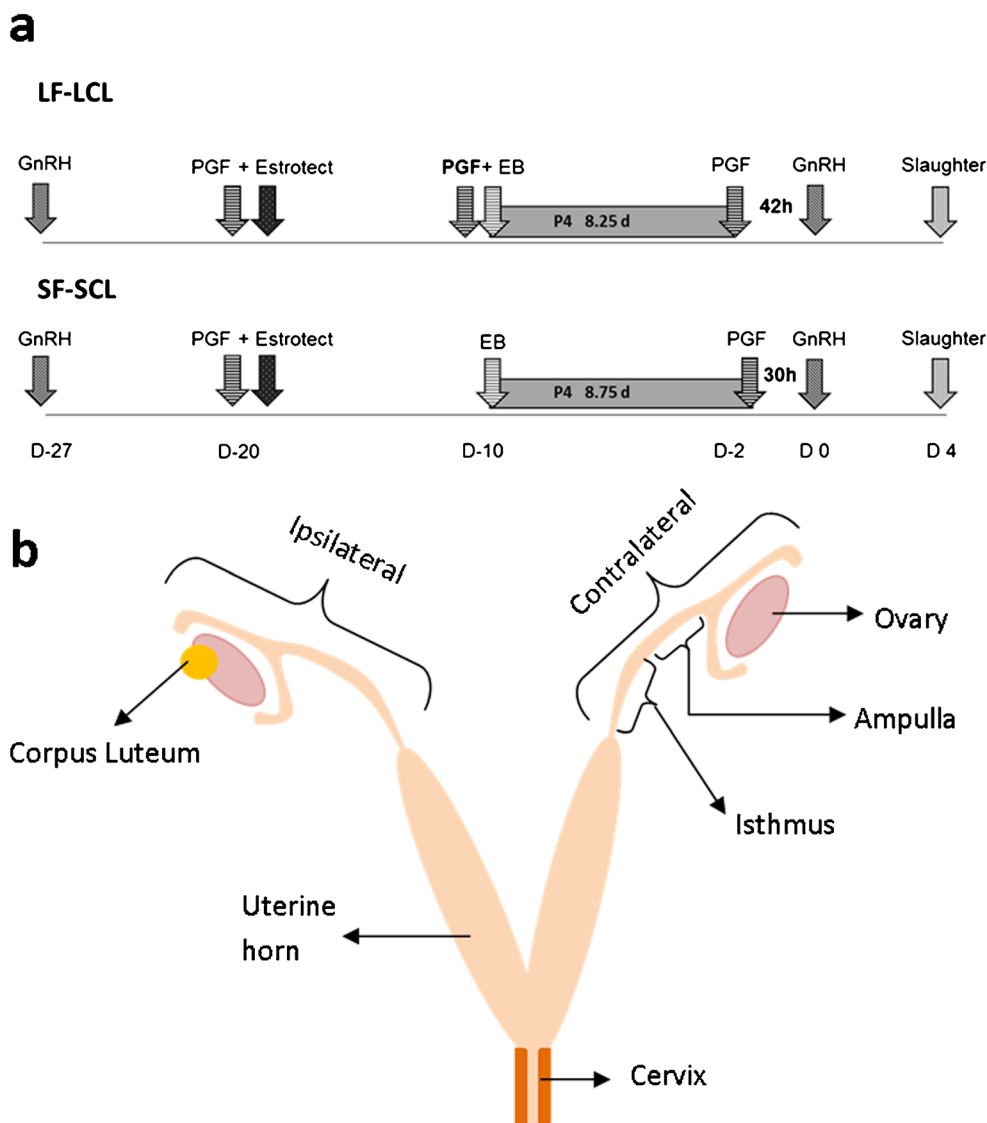


Fig. 1 Experimental model. **a** Hormonal manipulation protocol used in the present study. Animals ($n = 56$) were pre-synchronized by intramuscular injection of GnRH agonist and, 7 days later an injection of Prostaglandin F2 alpha (PGF) analog. At this day [day -20 (D-20)] animals received an ESTROTECT Heat detector device and estrus detection was performed twice daily from D-20 to D-10. All animals received a new intravaginal P4-releasing device on D-10 along with an intramuscular injection of 2 mg estradiol benzoate. Simultaneously, cows in the LF-LCL received an intramuscular injection of PGF. The P4 devices were removed on day -2, 42 h and 30 h before the GnRH

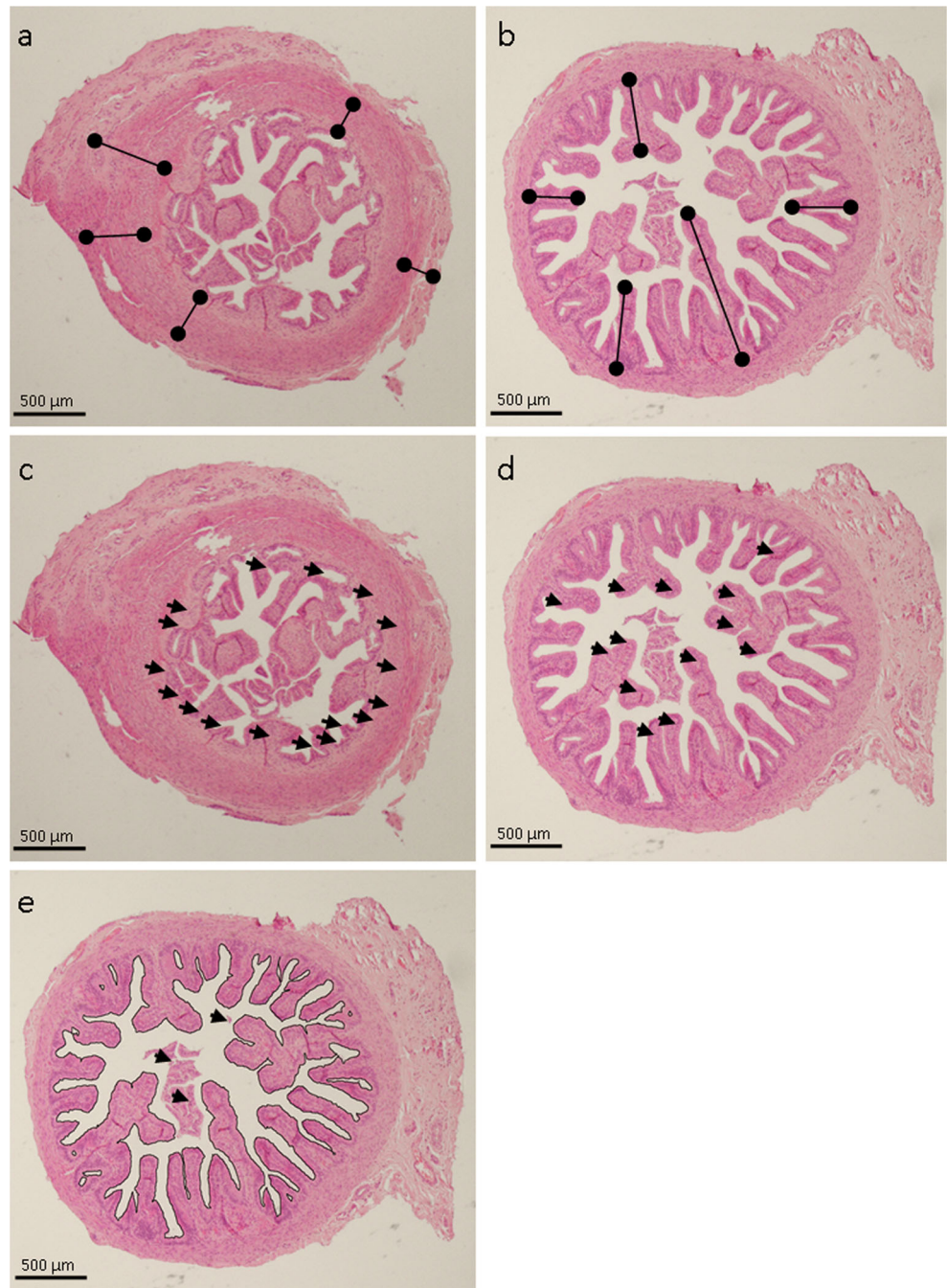
injection in the LF-LCL and the SF-SCL groups, respectively. All animals received a PGF injection at P4 device removal and a second PGF injection 6 h later. Ovulation was induced by an injection of GnRH agonist on D0. **b** Reproductive tract of the cow showing the local of the sample collection. Immediately after slaughter, the reproductive tract was removed, transported on ice and the ipsilateral and contralateral ovi-ducts were dissected. Later, ampulla and isthmus samples from each side were preserved for histological or molecular analysis

chromogen. The sections were counterstained with hematoxylin, dehydrated, cleared in xylene, and mounted on glass slides. Images were captured with a Nikon Eclipse TS100 microscope (Nikon, Tokyo, Japan) adapted to a digital camera (Moticam 580; Motic Asia, Hong Kong, China) and uploaded to the ImageJ software. Cells with a dense nuclear staining for KI67 were considered to be proliferating. The number of these cells was determined after counting a total of 500 cells per sample, using the “Cell Counter” plugin of ImageJ.

Transcript abundance by quantitative PCR

Frozen samples (≈ 20 mg) were ground in liquid nitrogen using a mortar and pestle and immediately mixed with buffer RLT from AllPrep[®] DNA/RNA/Protein Mini kit (No. 80004; Qiagen, São Paulo, São Paulo, Brazil), according to the manufacturer’s instructions. After homogenization with needle (18G) and syringe, the tissue suspension was centrifuged at 13,000g for 3 min for debris removal and the supernatant was

Fig. 2 The morphometric analysis performed on cross-sections of the isthmus (**a, c**) and ampulla (**b, d, e**) stained with hematoxylin-eosin. Measurements were taken of the height of muscular (**a**) and mucosa (**b**) layers, numbers of primary (**c**) and secondary folds (**d**), and the luminal epithelial perimeter (**e**). *Arrows* cell accumulations that were detached and not in direct contact with the tissue were ignored from the analysis



loaded in silica columns. Finally, the silica columns were eluted with 30 μL of RNase-free water and RNA was kept at $-80\text{ }^{\circ}\text{C}$. The concentration of total RNA extracts was measured using the NanoVue spectrophotometer (GE Healthcare). Total RNA (1 μg) was reverse transcribed (High Capacity cDNA Reverse Transcription Kit; Life Technologies, Carlsbad, CA, USA) according to the manufacturer's instructions. Briefly, samples were incubated at $25\text{ }^{\circ}\text{C}$ for 10 min, followed by incubation at $37\text{ }^{\circ}\text{C}$ for 2 h and reverse transcriptase inactivation at $85\text{ }^{\circ}\text{C}$ for 5 min and

storage at $-20\text{ }^{\circ}\text{C}$. The cDNA obtained was used for gene expression assays by qPCR. Step-One Plus (Life Technologies) with SYBR Green Chemistry was used for the amplification analysis. Primers were designed based on GenBank Ref-Seq mRNA sequences of target genes. Sequences were masked to remove repetitive sequences with RepeatMasker (<http://www.repeatmasker.org/>) (Smit et al. 1996,2010) and, then, the masked sequences were used to design primers using the PrimerQuest software (IDT1, <http://www.idtdna.com/primerquest/Home/Index>). Primers

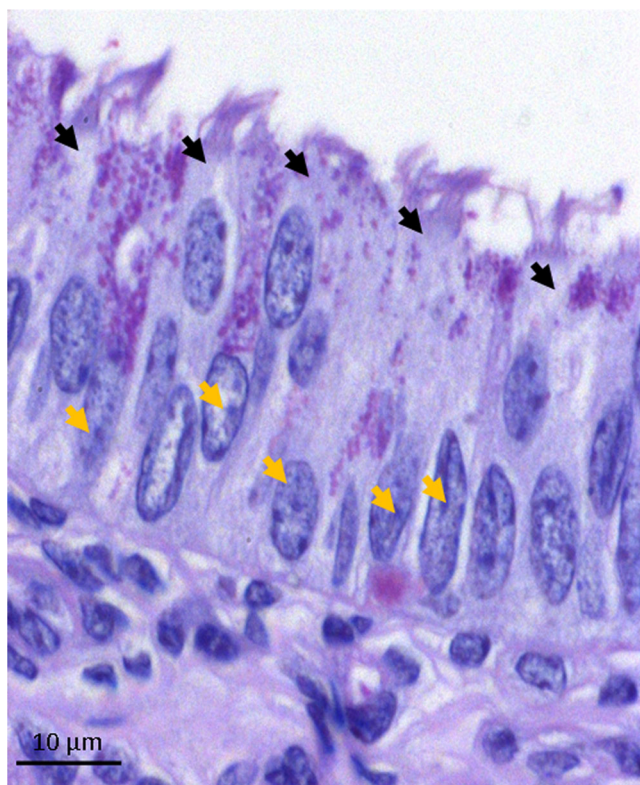


Fig. 3 Luminal epithelium of an ampulla cross-section stained with periodic acid-Schiff. *Black arrows* ciliated cells; *yellow arrows* secretory cells

characteristics were checked with Oligo Analyzer 3.1 software (IDT1, <http://www.idtdna.com/analyzer/Applications/OligoAnalyzer/>), while the specificity was compared by BLAST1 (NCBI, <http://blast.ncbi.nlm.nih.gov>). Quantitative PCR products from reactions containing designed primers were analyzed by agarose gel electrophoresis and SANGER sequencing, and identities were confirmed. Details of primers are provided in Table 1. Determination of qPCR efficiency and Cq (quantification cycle) values per sample were performed with LinRegPCR software (V2014.2; <http://linregpcr.nl/>). Cyclophilin A (*PPIA*) and Glyceraldehyde-3-Phosphate Dehydrogenase (*GAPDH*) were used as reference genes and their geometric mean was used to normalize the target transcript abundance values (Cq values). These reference genes were selected previously for stability of expression in oviduct tissues (Gonella-Díaz et al. 2015). The following candidate genes were selected because they were representative of ontology terms enriched in our previous study and considered relevant to oviductal biology: Branching morphogenesis [Bone morphogenetic protein 4 (*BMP4*); C-X-C chemokine receptor type 4 (*CXCR4*); Matrix metalloproteinase 14 (*MMP14*); Vinculin (*VCL*)], and cellular secretion [Cathepsin S (*CTSS*); C-Fos Induced Growth Factor (Vascular Endothelial Growth Factor D, *FIGF*); and Glucosidase Beta Acid (*GBA*); Heparanase (*HPSE*)].

Statistical analyses

In all statistical analyses performed, the animal was considered as the experimental unit. All data are reported as mean \pm standard error of the mean. Data was analyzed using Proc GLIMMIX of the SAS software (SAS 9.2; SAS Institute). The fixed effects of group (LF-LCL vs. SF-SCL), region (ampulla vs. isthmus), and side (ipsilateral vs. contralateral to the CL), as well as two-way interactions (group \times region, group \times side; region \times side) and the three-way interaction (group \times region \times side) were analyzed using a three-way nested ANOVA. Animal, animal within the group, animal within the interaction group \times region, and animal within the interaction group \times side were considered random effects. The model was adjusted in order to consider the distribution of the data of each dependent variable. The significance of the effects was determined using the type III sum of squares *F* test.

Results

Histological analysis

The thickness of the tunica mucosa ($P < 0.01$) and the tunica muscularis ($P < 0.01$) were different between regions (Fig. 4; Table 2). The ampulla has a thicker mucosa ($676.74 \pm 72.27 \mu\text{m}$) compared to the isthmus ($271.86 \pm 42.49 \mu\text{m}$), while the isthmus had a thicker tunica muscularis ($197.11 \pm 19.33 \mu\text{m}$) than the ampulla ($96.36 \pm 15.56 \mu\text{m}$). There was a significant three-way interaction in the number of primary mucosal folds (Fig. 5; Table 2; $P = 0.01$). The number of primary mucosal folds was always greater in the ampulla than the isthmus. However, in the ampulla it was greater for the LF-LCL group in the ipsilateral side, but not in the contralateral side. There were also no differences across all isthmus samples. The number of secondary folds was greater in the ampulla (15.16 ± 2.62 secondary folds) than in the isthmus (1.91 ± 2.30 secondary folds; $P < 0.01$). Due to the interest in studying the morphogenic processes, the ratio between the number of secondary folds and the number of primary folds was analyzed as a new dependent variable, called folding grade, for which a three-way interaction ($P = 0.03$) was detected (Fig. 5, Table 2). Although folding grade was always greater in the ampulla than the isthmus, in the ampulla it was greater for the LF-LCL group in the ipsilateral side, but not in the contralateral side, while it was similar across all isthmus samples. The luminal epithelial perimeter was affected by a group \times side interaction ($P = 0.06$). In the ipsilateral side, the luminal perimeter was similar for both groups in the isthmus, but significantly greater in the ampulla of cows in the LF-LCL group, while in the contralateral side mean perimeter was similar across regions and between groups. A three-way interaction

Table 1 Primer sequences of target and reference genes analyzed using qPCR

Target Gene	Gene Bank Number	Forward primer sequence(5'-3')	Reverse primer sequence (5'-3')	Primer efficiency (%)	Amplicon length (bp)
BMP4	NM_001045877.1	AGAGCGCAGTCATCCCGGAT	TCCAGATGTTCTTCGTGGTGGAAAGC	1.96	160
CTSS ^a	NM_001033615.2	AGAAGCCGTGGCCAATAAA	CTTCCCCTCAAGGTTACCATAG	2.10	157
CXCR4	NM_174301.3	AAAGTGACCCTGAGGACTTG AGTAG	CCGGAAGCAGGGTTCCTT	2.03	153
FIGF	NM_001101043.2	CACCTGCAGCTGTGAGGAC	GACATGGATGGGGAACTGGG	1.91	169
GBA	NM_001046421.2	GATTTCCCTTCGCCTCCGGT	AGGCATAGGATACTCCTCTCTGG	1.99	141
GAPDH ^a	NM_001034034.2	GCCATCAATGACCCCTTCAT	TGCCGTGGGTGGAATCA	1.93	69
HPSE ^a	NM_174082.2	CGGATTGTTGAGAAGATCAGA	AAGGTGTTGGACAGGAAGGG	1.92	94
MMP14	NM_174390.2	TGCCTACTGACAGGATTGA	GGGTATTCGCTTTCCACTATC	1.97	121
PPIA ^a	NM_178320.2	GCCATGGAGCGCTTTGG	CCACAGTCAGCAATGGTGATCT	2.02	64
VCL	NM_001191370.1	GCTGTTCAAGGGAGTAATAGG	TTCTGGCTTTGGGAAGAAATA	2.07	153

^a Primers for these genes have been previously reported in Gonella-Díaz et al. (2015)

was identified when the number of secretory cells was analyzed ($P = 0.01$; Fig. 6; Table 2). Similar to number of primary folds and folding grade, number of secretory cells was always greater in the ampulla than the isthmus; in the ampulla it was greater for the LF-LCL group in the ipsilateral side, but not in the contralateral side, while it was similar across all isthmus samples.

Staining for KI67 on the oviductal samples revealed the presence of proliferative activity in the luminal epithelium of all samples. After KI-67-positive nuclei counting, a significant effect of region ($P = 0.03$) and group ($P = 0.02$; Fig. 6) was observed. The proliferation activity was stronger in the ampulla (7.72 ± 2.22 KI67-positive cells) than in the isthmus (0.92 ± 0.34 cells KI67 positive cells) and in the LF-LCL group (7.60 ± 1.90 KI67-positive cells) than in the SF-SCL group (1.03 ± 0.66 KI67-positive cells).

Gene expression

The P values of fixed effects and their interactions for the transcripts abundance of candidate genes are shown on Table 3. A three-way interaction was detected for transcript abundance of *GBA* ($P = 0.02$; Fig. 7) and *CTSS* ($P = 0.01$; Fig. 7). While *GBA* transcript abundance in the SF-SCL group was less in the isthmus than in the ampulla in both sides, abundance in the LF-LCL animals slightly increased in the ipsilateral isthmus and slightly decreased in the contralateral isthmus, compared to the respective ampullae. *CTSS* transcript abundance was up-regulated in the ipsilateral isthmus and the contralateral ampulla of the LF-LCL group. Group means were similar in the ipsilateral ampulla and in the contralateral isthmus.

There was a region \times side interaction on the transcript abundance of *MMP14* ($P = 0.04$; Fig. 7). Abundance was greater in the contralateral isthmus compared with the other regions, but similar between regions in the ipsilateral oviduct.

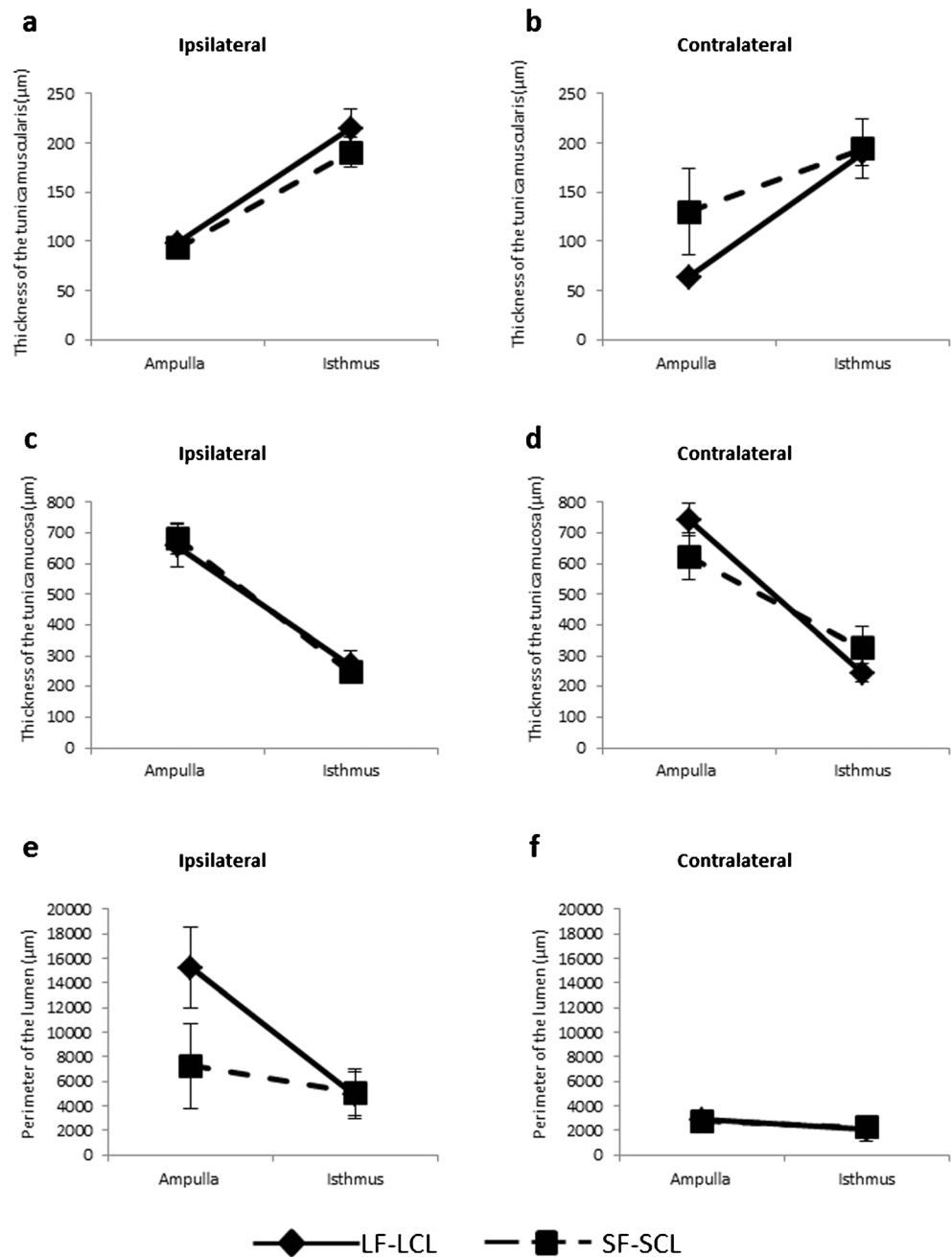
The group \times region interaction of *VCL* transcript abundance ($P = 0.09$; Fig. 7) indicated that, while group means were similar in the ampulla, the LF-LCL group presented up-regulated *VCL* expression in the isthmus.

There was a significant effect of the side in the *BMP4* ($P = 0.02$; Fig. 8) and *FIGF* ($P = <0.01$; Fig. 8) transcript abundance, both of them being up-regulated in the contralateral side. The transcript abundance of *CXCR4* ($P = 0.09$; Fig. 8), *FIGF* ($P = 0.01$) and, *HPSE* ($P = < 0.01$; Fig. 8) was affected by region; transcripts were more abundant in the ampulla than in the isthmus. *BMP4* transcript abundance was greater in the LF-LCL group ($P = 0.05$).

Discussion

The positive role of the oviduct in embryo quality is well accepted. For example, it is clear that quality and developmental potential of in vivo-produced embryos is greater than in vitro-produced embryos (Rizos et al. 2002a, 2002b, 2002c). However, there is a poor understanding of cellular and molecular mechanisms that affect oviduct functions to impact embryo development and quality. Previous assessment of the oviductal transcriptome have elucidated a number of mechanisms regulated by the periovulatory endocrine milieu, i.e., proestrus and estrus increase in E2 and diestrus increase in P4 concentrations, potentially involved in oviductal function (Gonella-Díaz et al. 2015). Such pathways included branching morphogenesis, cellular proliferation, and secretion. More importantly, genes in these pathways were up-regulated in the LF-LCL group, associated with a greater receptivity to the embryo. It was expected that, in response to pre-ovulatory E2, the oviduct initiates morphogenic and proliferative processes, resulting in invasion of the epithelium into the lumen and the modifying of the number of secretory

Fig. 4 Values (mean \pm SEM) of the thick of the tunica muscularis (a, b) and mucosa (c, d) and perimeter of the lumen (e, f) in ipsilateral or contralateral to the CL oviducts for cows of the LF-LCL and SF-SCL groups ($n = 7$ animals per group)



cells, finally increasing the functional epithelial area. The main objective of this study was to compare the morphology, gene expression, and cellular proliferation of two regions (ampulla and isthmus) of the ipsilateral and contralateral oviducts between groups of cows showing distinctly different periovulatory endocrine milieus associated with greater (LF-LCL group) or lower (SF-SCL group) fertility.

Growth and ovulation of a larger follicle stimulate development of the oviductal secretory mucosa. In the present study, the number of primary folds, folding grade and the luminal epithelium perimeter were greater in the oviduct of animals of the LF-LCL group. In the endometrium, after an E2

stimulus, cells are stimulated to proliferate and endometrial glands reorganize, resulting in greater glandular epithelium area (Gray et al. 2001; Wang et al. 2007). The oviductal mucosa, due to structural simplicity and its lack of glands, depends mainly on the luminal epithelial cells to synthesize oviductal fluid (Abe 1996; Leese 1988.). It is expected that a greater secretory capacity is better able to provide molecules important to support embryo development (Aviles et al. 2010; Hunter 1998; Simintiras et al. 2016). As described previously, variables associated with the secretory mucosa were better developed in the ampulla than in the isthmus (Buhi et al. 1991; Buhi et al. 1992). Interestingly, mucosal development

Table 2 *P* value ($Pr > F$) of the fixed effects: group (LF-LCL vs. SF-SCL), region (ampulla vs. isthmus), and side (ipsilateral vs. contralateral) with their respective double and triple interactions for the morphological variables evaluated

Dependent variable	Group	Region	Side	Group × region	Group × side	Region × side	Group × region × side
Thick of the tunica mucosa (μm)	NS	<0.01	NS	NS	NS	NS	NS
Thick of the tunica muscularis (μm)	NS	<0.01	NS	NS	0.09	NS	NS
Number of primary mucosa folds	0.09	<0.01	NS	0.03	NS	0.09	0.01
Number of secondary mucosal folds	NS	<0.01	NS	NS	NS	NS	NS
Folding grade	NS	<0.01	NS	NS	NS	NS	0.03
Luminal epithelium perimeter (μm)	NS	<0.01	NS	NS	0.04	0.08	0.06
Ratio of secretory cells	0.02	<0.01	NS	NS	<0.01	<0.01	0.01
Number of Ki67 positive cells	0.02	0.03	NS	NS	NS	NS	NS

Statistically significant differences were determined by three-way nested ANOVA where NS depicts not statistically significant

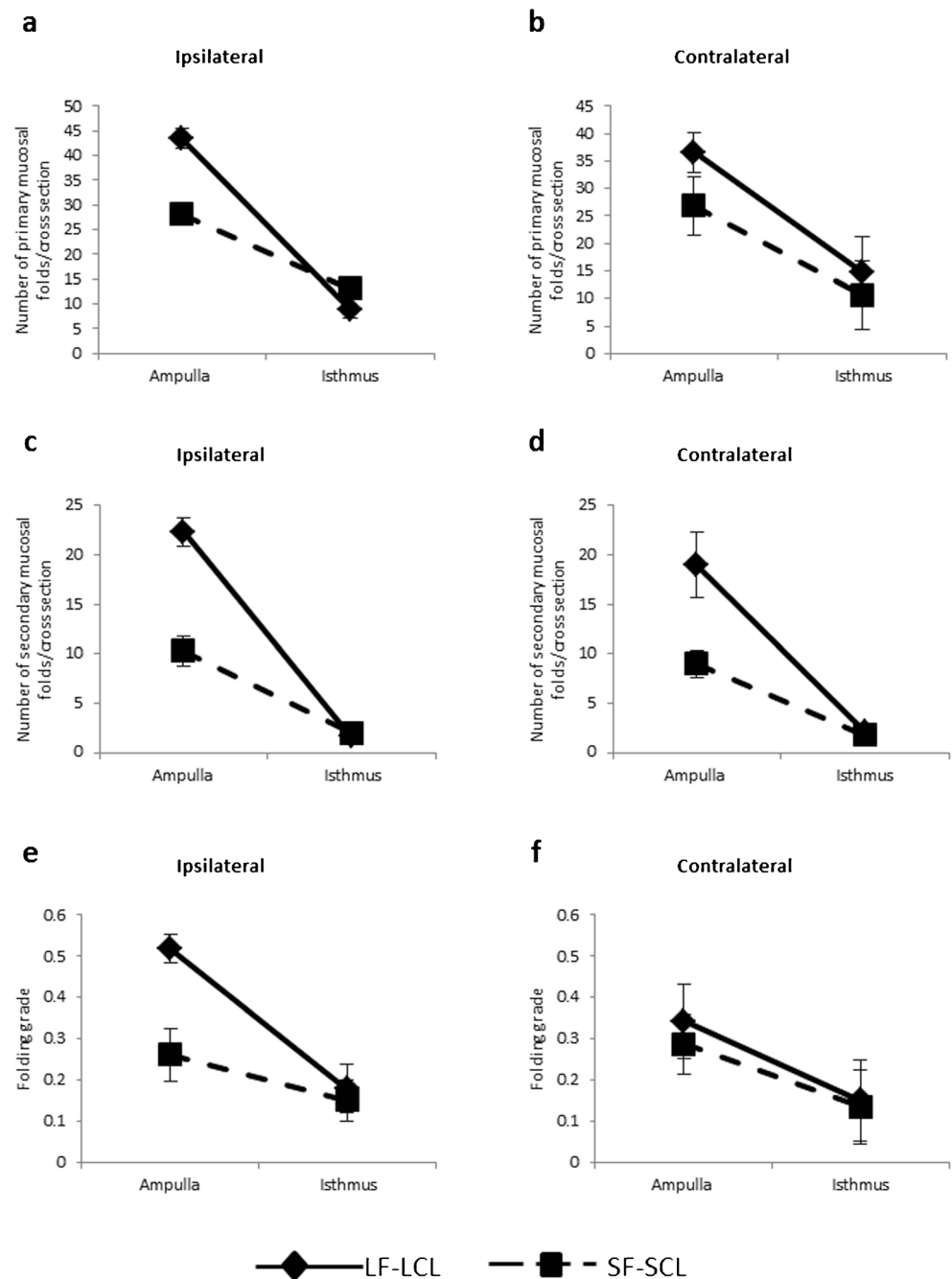
was also greater in the ipsilateral compared to the contralateral oviduct. Vascular arrangements in the cranial portion of the uterus and the oviduct direct greater amounts of gonadal steroids to this region of the reproductive tract. Thus, the side ipsilateral to the pre-ovulatory follicle and the subsequent CL is exposed to a greater concentration of sex-steroids (Hunter et al. 1983; Wijayagunawardane et al. 1996, 1998). This may explain the increased folding of the luminal epithelium of the ipsilateral in comparison to the contralateral side. Morphology of the oviduct compartments was consistent with previous transcriptomic data, indicating enrichment of transcripts related to branching morphogenesis in the oviduct of LF-LCL cows (Gonella-Diaz et al. 2015). Taking these findings together, it was hypothesized that the greater luminal epithelial surface developed by the LF-LCL cows would result in a greater secretory capacity. However, because not all of the epithelial cells secrete components of the oviductal fluid, it was necessary to measure the numbers of secretory cells.

Growth and ovulation of a larger follicle increased the number of secretory cells and KI67-positive proliferating cells. The ampulla of LF-LCL cows has a greater amount of both secretory and proliferating cells (Fig. 6; Table 2). The secretory cells actively produce and secrete specific glycoproteins into the lumen and their secretions form the oviductal fluid (Aguilar and Reyley 2005; Eriksen et al. 1994; Leese 1988). These cells are more abundant in the ampulla and, during the estrous cycle, the number of secretory cells varies. Indeed, during the follicular phase, the number of secretory cells, as well as the volume of oviductal fluid, increase (Ayen et al. 2012; Ito et al. 2016; Leese 1988). Therefore, it can be assumed that cows ovulating larger follicles would exhibit greater proliferation rates and, therefore, have more secretory cells therein producing more oviductal fluid. Also, the KI67-positive cells were almost ten times more frequent in the LF-LCL group than in the SF-SCL group. These results are in agreement with a recent study published by Ito et al. (2016), who concluded that the proportions of ciliated and secretory

epithelial cells change during the estrous cycle and that only the secretory cells proliferate. The data also suggest that the remodeling of the bovine oviductal epithelium provides the optimal environment for gamete transport, fertilization, and embryonic development. Furthermore, remodeling is mainly regulated by proliferation of secretory cells.

Morphological changes induced by growth and ovulation of a larger follicle were not associated with changes in abundance of selected transcripts. In this study, regulation of transcript abundance among groups, regions and sides was complex. In the ipsilateral ampullae, the abundance of all transcripts studied was similar between groups. It is possible that transcript regulation associated with the morphological differences between groups, described above for that region, occurred at an earlier point in time not sampled in the present study. Conversely, despite the absence of morphological changes between groups in the ipsilateral isthmus, there was a greater abundance of transcripts associated with secretion (*CTSS*, *GBA*) and branching morphogenesis (*BMP4*, *MMP14*) in cows from the LF-LCL group. On D4, it is expected that the embryo will be in the isthmus, in transit to the uterus (Kolle et al. 2009). Thus, morphological changes observed in the ampulla may be important for processes that occurred prior to the moment samples were collected, such as fertilization, the initial embryo divisions and transport to the isthmus. The D4 isthmus role is to support the final embryo divisions before entering the uterus and to transport the embryo. Based on the isthmus morphological variables that we measured, changes in the secretory epithelium were probably not associated with a functional advantage for cows on the LF-LCL group. Conversely, changes in transcript abundance are suggestive of LF-LCL-stimulated secretory activity per individual pre-existing cell because there was no evidence of proliferation. Furthermore, tissue remodeling involving *MMP14* and *BMP4* may be critical to transport the embryo to the uterus. A recent study in which embryos were cocultured with bovine oviductal epithelial cells (BOEC)

Fig. 5 Values of the number of primary (a, b) and secondary (c, d) mucosal folds, and folding grade (e, f) in ipsilateral or contralateral to the CL oviducts for cows of the LF-LCL and SF-SCL groups ($n = 7$ animals per group)

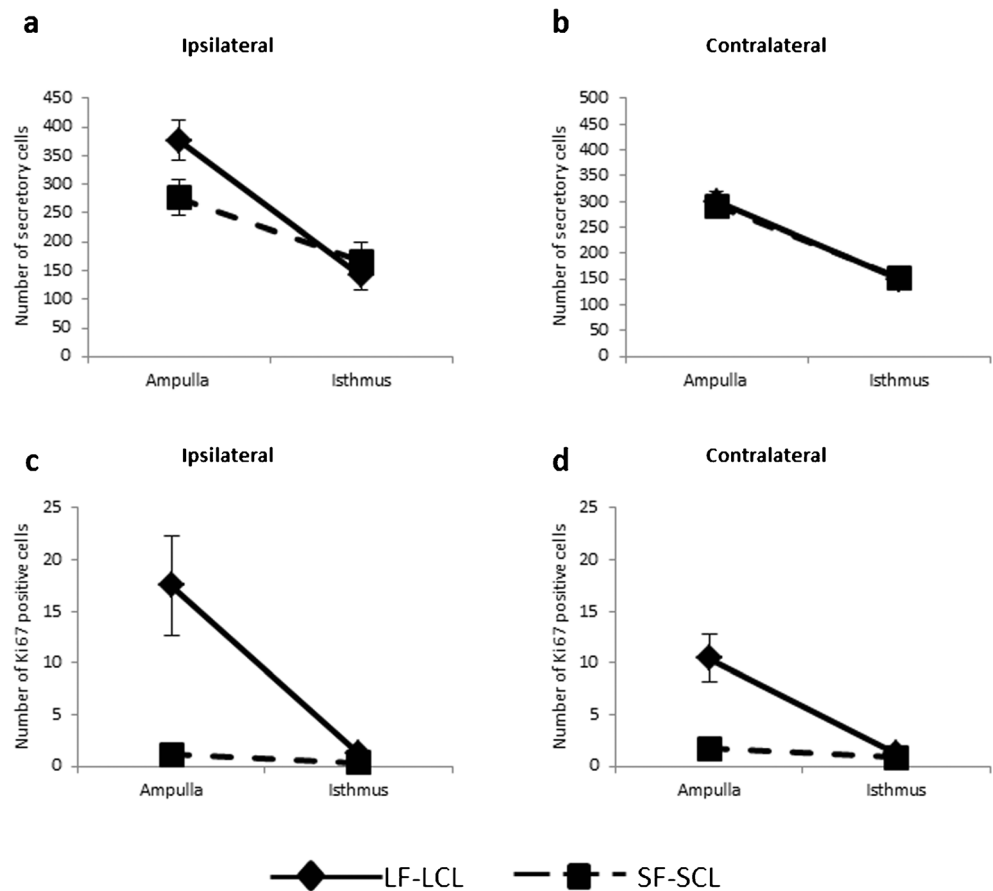


demonstrated that embryo–oviduct interaction *in vitro* induces specific changes in the transcriptional levels of BMP signaling (García et al. 2017). Specifically, they found a reduction in the expression levels of BMP signaling in the BOEC, while they increased in the early embryo. So, it could be presumed that the reduction in the BMP signaling is important for the embryo during the first stages of its development. In another study in which BOEC were cultured in a polarized system with a high concentration of non-esterified fatty acids (NEFA), it has been suggested that the oviduct serves as a gatekeeper which may actively alter the environment in which

the embryo development takes place (Jordaens et al. 2017). All this together could indicate that it is not only necessary that the oviductal cells provide the correct environment for embryo development but also that these cells have the capacity to respond to embryo signals and to systemic conditions.

In summary, exposure to greater proestrus–estrus concentrations of E2 and early diestrus concentrations of P4 dramatically changes ampullary morphology to a highly secretory phenotype that may be critical to support embryo early development. Additional analyses to evaluate whether these morphological and gene expression differences are associated

Fig. 6 Number (mean ± SEM) of secretory cells (a, b) and Ki67 positive cells (c, d) in ipsilateral or contralateral to the CL oviducts of cows of the LF-LCL and SF-SCL groups ($n = 7$ animals per group)



with greater bioavailability of nutrients and growth factors to the embryo are necessary. In the isthmus, similar morphological changes were not regulated, indicating that they were not required to support isthmus function. However, changes in critical transcript abundance suggest that this region is also under sex-steroid regulation, which is further supported by the detection of cognate receptors reported earlier. Future experiments are warranted to determine the role of the

periovalutary endocrine milieu on tissue remodeling. Collectively, these observations may help to explain the greater fertility of cows ovulating larger follicles and developing larger CLs. In conclusion, the present data provide functional connections between a fertility model and the oviduct transcriptome in beef cattle. We propose that sex-steroids act in an oviduct region-specific fashion to support early embryo development.

Table 3 P value ($Pr > F$) of the fixed effects: group (LF-LCL vs. SF-SCL), region (ampulla vs. isthmus), and side (ipsilateral vs. contralateral) with their respective double and triple interactions for the abundance of transcripts evaluated by qPCR

Dependent variable	Group	Region	Side	Group × Region	Group × Side	Region × Side	Group × Region × Side
BMP4	0.05	NS	0.02	NS	NS	NS	NS
CTSS	0.03	<0.01	0.03	NS	NS	NS	0.01
CXCR4	NS	0.09	NS	NS	NS	NS	NS
FIGF	NS	0.01	<0.01	NS	NS	NS	NS
GBA	0.06	0.02	NS	0.02	NS	0.03	0.02
HPSE	NS	<0.01	NS	NS	NS	NS	NS
MMP14	NS	<0.01	0.07	NS	NS	0.04	NS
VCL	0.09	<0.01	NS	0.09	NS	NS	NS

Statistically significant differences were determined by three-way nested ANOVA where NS depicts not statistically significant

Fig. 7 Transcript abundance (mean \pm SEM) of CTSS (a, b), GBA (c, d), MMP14 (e, f), and VCL (g, h). Gene expression was normalized to PPIA and GAPDH in the oviducts ipsilateral and contralateral to the CL from beef cows synchronized to ovulate a large (LF-LCL) or small follicles (SF-SCL) an day 4 of the estrous cycle ($n = 7$ animals per group)

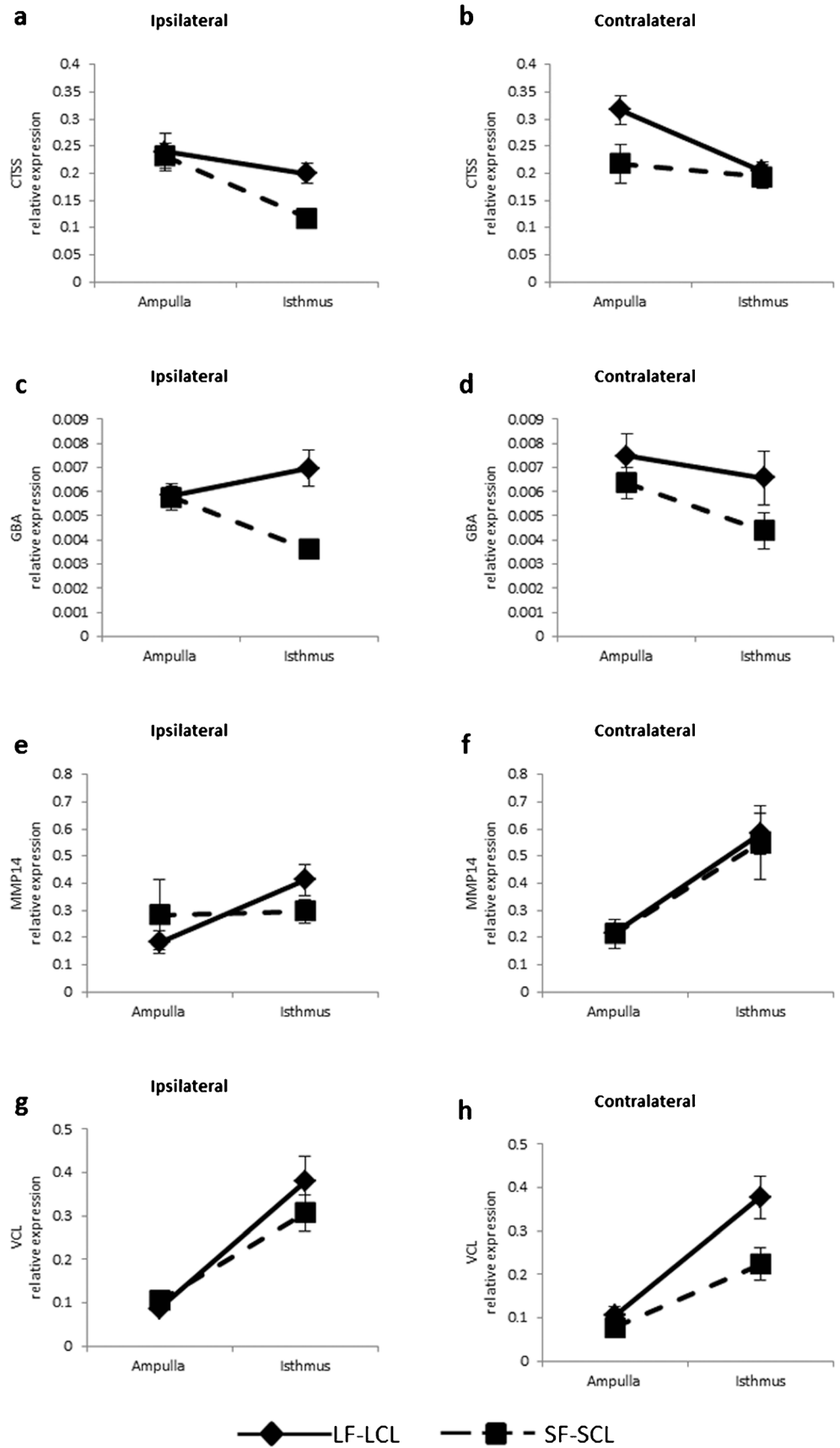
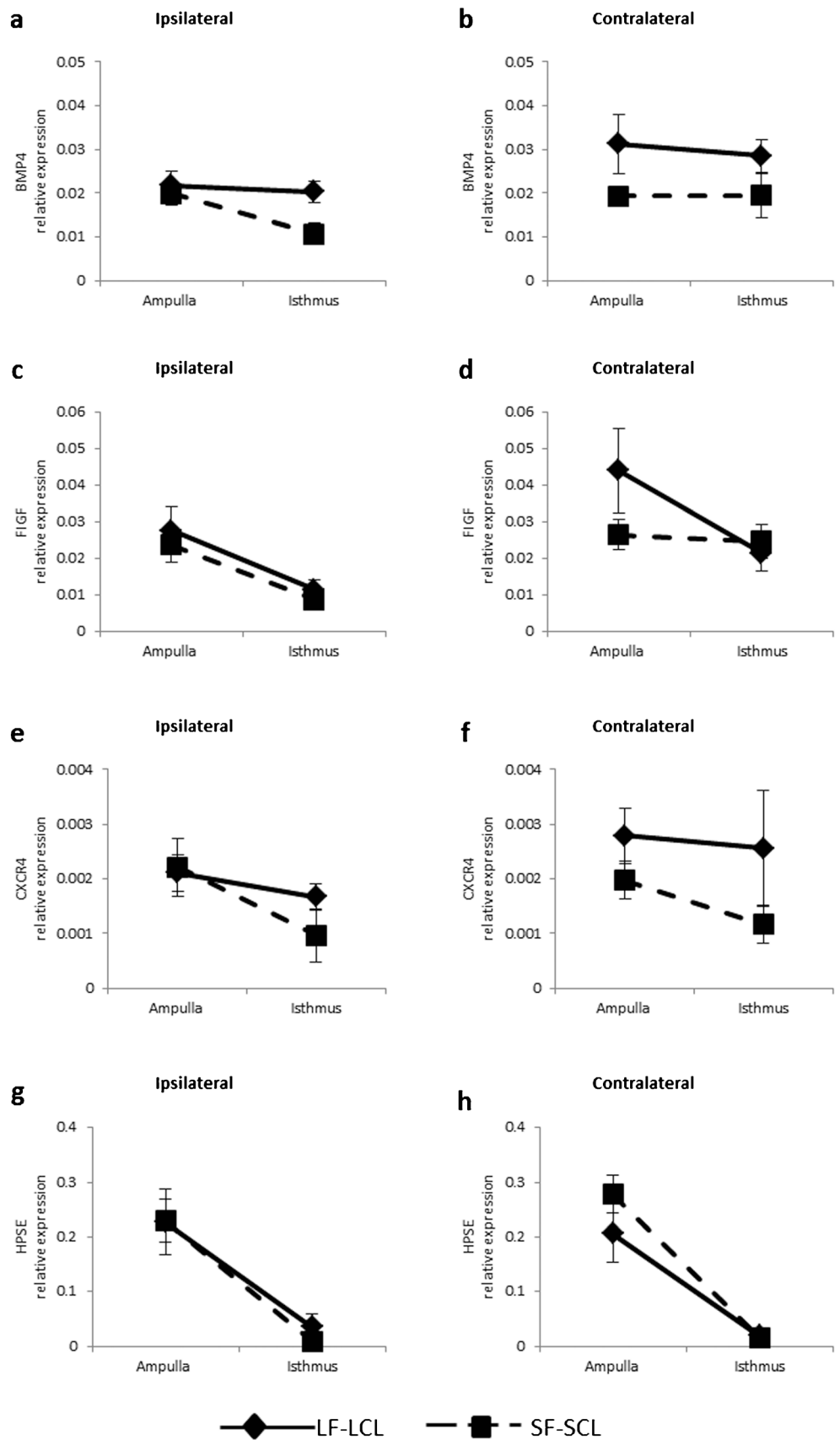


Fig. 8 Transcript abundance (mean ± SEM) of BMP4 (**a, b**), FIGF (**c, d**), CXCR4 (**e, f**), and HPSE (**g, h**). Gene expression was normalized to PPIA and GAPDH in the oviducts ipsilateral and contralateral to the CL from beef cows synchronized to ovulate a large (LF-LCL) or small follicles (SF-SCL) on day 4 of the estrous cycle ($n = 7$ animals per group)



Acknowledgements The authors thank M. R. França, R. S. Ramos, E. Lopes, E. R. Araujo, M. L. Oliveira, and C. M. Membrive for technical assistance; and the administration of the Pirassununga campus of the University of São Paulo for assistance in animal handling.

Compliance with ethical standards

Conflict of interest The authors declare that there is no conflict of interest that could be perceived as prejudicing the impartiality of the research reported.

Funding This research was funded by: Coordenação de Aperfeiçoamento de Pessoal de Nível Superior (CAPES) PEC-PG program: AMGD grant number 15068–12-9; Conselho Nacional de Desenvolvimento Científico e Tecnológico (CNPq); Fundação de Amparo à Pesquisa do Estado de São Paulo (FAPESP): MB grant number 2011/03226–4. The funders had no role in study design, data collection and analysis, decision to publish, or preparation of the manuscript.

References

- Abe H (1996) The mammalian oviductal epithelium: regional variations in cytological and functional aspects of the oviductal secretory cells. *Histol Histopathol* 11:743–768
- Agduhr E (1927) Studies on the structure and development of the bursa ovarica and the tuba uterina in the mouse. *Acta Zool* 8:1–133
- Aguilar J, Reyley M (2005) The uterine tubal fluid: secretion, composition and biological effects. *Anim Reprod* 2:91–105
- Ahumada CJ, Salvador I, Cebrian-Serrano A, Lopera R, Silvestre MA (2013) Effect of supplementation of different growth factors in embryo culture medium with a small number of bovine embryos on in vitro embryo development and quality. *Animal* 7:455–462
- Ashworth CJ, Sales DI, Wilmut I (1989) Evidence of an association between the survival of embryos and the periovulatory plasma progesterone concentration in the ewe. *J Reprod Fertil* 87:23–32
- Aviles M, Gutierrez-Adan A, Coy P (2010) Oviductal secretions: will they be key factors for the future ARTs? *Mol Hum Reprod* 16:896–906
- Ayen E, Shahrooz R, Kazemie S (2012) Histological and histomorphometrical changes of different regions of oviduct during follicular and luteal phases of estrus cycle in adult Azarbaijan buffalo. *Iran J Vet Res* 13:42–48
- Bacha WJ, Bacha LM (2012) Color atlas of veterinary histology, 3rd edn. Wiley-Blackwell, New York
- Besenfelder U, Havlicek V, Brem G (2012) Role of the oviduct in early embryo development. *Reprod Domest Anim* 47:156–163
- Brower L, Anderson E (1969) Cytological events associated with the secretory process in the rabbit oviduct. *Biol Reprod* 1:130–148
- Buhi WC, Bazer FW, Alvarez IM, Miranda MA (1991) In vitro synthesis of oviductal proteins associated with estrus and 17 beta-estradiol-treated ovariectomized ewes. *Endocrinology* 128:3086–3095
- Buhi WC, Ashworth CJ, Bazer FW, Alvarez IM (1992) In vitro synthesis of oviductal secretory proteins by estrogen-treated ovariectomized gilts. *J Exp Zool* 262:426–435
- Buhi WC, Alvarez IM, Kouba AJ (2000) Secreted proteins of the oviduct. *Cells Tissues Organs* 166:165–179
- Chanrota M, Guoa Y, Dalina AM, Persson B, Båge R, Svensson A, Gustafsson H, Humblot P (2017) Dose related effects of LPS on endometrial epithelial cell populations from dioestrus cows. *Anim Reprod Sci* 177:12–24
- Demetrio DG, Santos RM, Demetrio CG, Vasconcelos JL (2007) Factors affecting conception rates following artificial insemination or embryo transfer in lactating Holstein cows. *J Dairy Sci* 90:5073–5082
- Donnez J, Casanas-Roux F, Caprasse J, Ferin J, Thomas K (1985) Cyclic changes in ciliation, cell height, and mitotic activity in human tubal epithelium during reproductive life. *Fertil Steril* 43:554–559
- Eriksen T, Terkelsen O, Hyttel P, Greve T (1994) Ultrastructural features of secretory-cells in the bovine oviduct epithelium. *Anat Embryol* 190:583–590
- Gandolfi F, Brevini TAL, Richardson L, Brown CR, Moor RM (1989) Characterization of proteins secreted by sheep oviduct epithelial-cells and their function in embryonic-development. *Development* 106:303–312
- García EV, Hamdi M, Barrera AD, Sánchez-Calabuig MJ, Gutiérrez-Adán A, Rizos D (2017) Bovine embryo-oviduct interaction in vitro reveals an early cross talk mediated by BMP signaling. *Reproduction* 153:631–643
- Gonella-Díaza A, Andrade S, Sponchiado M, Pugliesi G, Mesquita F, Van Hoecck V, Strefezzi R, Gasparin G, Coutinho L, Binelli M (2015) Size of the ovulatory follicle dictates spatial differences in the oviductal transcriptome in cattle. *PLoS ONE* 10:e0145321
- Gray CA, Bartol FF, Tarleton BJ, Wiley AA, Johnson GA, Bazer FW, Spencer TE (2001) Developmental biology of uterine glands. *Biol Reprod* 65:1311–1323
- Hunter RH (1998) Have the fallopian tubes a vital role in promoting fertility? *Acta Obstet Gynecol Scand* 77:475–486
- Hunter RH (2012) Components of oviduct physiology in eutherian mammals. *Biol Rev Camb Philos Soc* 87:244–255
- Hunter RH, Cook B, Poyser NL (1983) Regulation of oviduct function in pigs by local transfer of ovarian steroids and prostaglandins: a mechanism to influence sperm transport. *Eur J Obstet Gynecol Reprod Biol* 14:225–232
- Ito S, Kobayashi Y, Yamamoto Y, Kimura K, Okuda K (2016) Remodeling of bovine oviductal epithelium by mitosis of secretory cells. *Cell Tissue Res* 366:403–410
- Jordaens L, Van Hoecck V, Maillo V, Gutierrez-Adan A, Marei WFA, Vlaeminck B, Thys S, Sturmey RG, Bols PEJ, Leroy JLMR (2017) Maternal metabolic stress may affect oviduct gatekeeper function. *Reproduction* 153:759–773
- Kenngott RA, Sinowatz F (2007) Prenatal development of the bovine oviduct. *Anat Histol Embryol* 36:272–283
- Kolle S, Dubielzig S, Reese S, Wehrend A, König P, Kummer W (2009) Ciliary transport, gamete interaction, and effects of the early embryo in the oviduct: ex vivo analyses using a new digital videomicroscopic system in the cow. *Biol Reprod* 81:267–274
- Konishi I, Fujii S, Parmley TH, Mori T (1987) Development of ciliated cells in the human fetal oviduct: an ultrastructural study. *Anat Rec* 219:60–68
- Leese HJ (1988) The formation and function of oviduct fluid. *J Reprod Fertil* 82:843–856
- McDaniel JW, Scalzi H, Black D (1968) Influence of ovarian hormones on histology and histochemistry of the bovine oviduct. *J Dairy Sci* 51:754–761
- Mesquita FS, Pugliesi G, Scolari SC, Franca MR, Ramos RS, Oliveira M, Papa PC, Bressan FF, Meirelles FV, Silva LA, Nogueira GP, Membrive CM, Binelli M (2014) Manipulation of the periovulatory sex steroid milieu affects endometrial but not luteal gene expression in early diestrus Nelore cows. *Theriogenology* 81:861–869
- Mesquita FS, Ramos RS, Pugliesi G, Andrade SC, Van Hoecck V, Langbein A, Oliveira ML, Gonella-Díaza AM, Gasparin G, Fukumasu H, Pulz LH, Membrive CM, Coutinho LL, Binelli M (2015) The receptive endometrial transcriptomic signature indicates an earlier shift from proliferation to metabolism at early Diestrus in the cow. *Biol Reprod* 93:52
- Mokhtar DM (2015) Microscopic and histochemical characterization of the bovine uterine tube during the follicular and luteal phases of estrous cycle. *J Microsc Ultrastruct* 3:44–52
- Morris D, Diskin M (2008) Effect of progesterone on embryo survival. *Animal* 2:1112–1119

- Peres RF, Claro I Jr, Sa Filho OG, Nogueira GP, Vasconcelos JL (2009) Strategies to improve fertility in *Bos indicus* postpubertal heifers and non-lactating cows submitted to fixed-time artificial insemination. *Theriogenology* 72:681–689
- Pugliesi G, Santos FB, Lopes E, Nogueira É, Maio JR, Binelli M (2016) Improved fertility in suckled beef cows ovulating large follicles or supplemented with long-acting progesterone after timed-AI. *Theriogenology* 85:1239–1248
- Restall BJ (1966) Histological observations on the reproductive tract of the ewe. *Aust J Biol Sci* 19:673–686
- Rizos D, Fair T, Papadopoulos S, Boland MP, Lonergan P (2002a) Developmental, qualitative, and ultrastructural differences between ovine and bovine embryos produced in vivo or in vitro. *Mol Reprod Dev* 62:320–327
- Rizos D, Lonergan P, Boland MP, Arroyo-Garcia R, Pintado B, de la Fuente J, Gutierrez-Adan A (2002b) Analysis of differential messenger RNA expression between bovine blastocysts produced in different culture systems: implications for blastocyst quality. *Biol Reprod* 66:589–595
- Rizos D, Ward F, Duffy P, Boland MP, Lonergan P (2002c) Consequences of bovine oocyte maturation, fertilization or early embryo development in vitro versus in vivo: implications for blastocyst yield and blastocyst quality. *Mol Reprod Dev* 61:234–248
- Simintiras CA, Fröhlich T, Sathyapalan T, Arnold GJ, Ulbrich SE, Leese HJ, Sturmey RG (2016) Modelling oviduct fluid formation in vitro. *Reproduction* 153:23–33
- Smit A, Hubley R, Green P (1996–2010) RepeatMasker Open-3.0. <http://www.repeatmasker.org>
- Vasconcelos JLM, Sartori R, Oliveira HN, Guenther JG, Wiltbank MC (2001) Reduction in size of the ovulatory follicle reduces subsequent luteal size and pregnancy rate. *Theriogenology* 56:307–314
- Wang CK, Robinson RS, Flint APF, Mann GE (2007) Quantitative analysis of changes in endometrial gland morphology during the bovine oestrous cycle and their association with progesterone levels. *Reproduction* 134:365–371
- Wetscher F, Havlicek V, Huber T, Muller M, Brem G, Besenfelder U (2005) Effect of morphological properties of transferred embryonic stages on tubal migration implications for in vivo culture in the bovine oviduct. *Theriogenology* 64:41–48
- Wijayagunawardane MPB, Cerbito WA, Miyamoto A, Acosta TJ, Takagi M, Miyazawa K, Sato K (1996) Oviductal progesterone concentration and its spatial distribution in cyclic and early pregnant cows. *Theriogenology* 46:1149–1158
- Wijayagunawardane MPB, Miyamoto A, Cerbito WA, Acosta TJ, Takagi M, Sato K (1998) Local distributions of oviductal estradiol, progesterone, prostaglandins, oxytocin and endothelin-1 in the cyclic cow. *Theriogenology* 49:607–618
- Yoshioka S, Abe H, Sakumoto OK (2013) Proliferation of luteal steroidogenic cells in cattle. *PLoS ONE* 8:e84186